



PNMA5 knockdown suppresses the proliferation, invasion, and metastasis of epithelial ovarian cancer cells

Haifeng Qiao^{1,2,3#}, Jinwei Liu^{1,3,4#}, Zhixia Yang³, Leilei Gao^{3,4}, Xiaolan Zhang³, Guangping Lu⁵, Yinglei Liu², Manhua Liu², Xiaoyan Ying¹, Dong Zhang³

¹Department of Obstetrics and Gynecology, The Second Affiliated Hospital of Nanjing Medical University, Nanjing 210029, China; ²Department of Obstetrics and Gynecology, The Second Affiliated Hospital of Nantong University, Nantong 226001, China; ³State Key Lab of Reproductive Medicine, Nanjing Medical University, Nanjing 211116, China; ⁴Department of Gynecology, Zhejiang Provincial People's Hospital, Hangzhou 310000, China; ⁵Department of Oncology, The Dongtai Affiliated Hospital of Nantong University, Dongtai 224200, China

Contributions: (I) Conception and design: X Ying, D Zhang; (II) Administrative support: D Zhang, Z Yang; (III) Provision of study materials or patients: H Qiao, Y Liu, M Liu; (IV) Collection and assembly of data: H Qiao, J Liu, Z Yang; (V) Data analysis and interpretation: H Qiao, L Gao, X Zhang, G Lu; (VI) Manuscript writing: All authors; (VII) Final approval of manuscript: All authors.

#These authors contributed equally to this work.

Correspondence to: Xiaoyan Ying. Department of Obstetrics and Gynecology, The Second Affiliated Hospital of Nanjing Medical University, Nanjing 210029, China. Email: xiaoyanying_efy@163.com; Dong Zhang. State Key Lab of Reproductive Medicine, Nanjing Medical University, Nanjing 211116, China. Email: dong.ray.zhang@njmu.edu.cn.

Background: Ovarian cancer is a severe gynecological malignancy. Paraneoplastic Ma antigen 5 (PNMA5) is a confirmed tumor onconeural antigen, which has been screened as a female fertility factor. PNMA5 overexpression might serve as a marker of poor prognosis in colon cancer. Our earlier study showed that PNMA5 was essential for meiosis in mouse oocytes. In this study, we investigate the role and probable mechanism of PNMA5 in the occurrence and development of epithelial ovarian cancer (EOC).

Methods: Immunohistochemistry and western blot analyses were used to verify PNMA5 overexpression in clinical EOC tissues and EOC cell line HO8910. A specific siRNA was used to reduce PNMA5 levels, and several proliferation and migration-related indexes were assessed. We also examined mitochondria, microfilaments, and several essential kinases.

Results: We found that the expression of PNMA5 in EOC tissues was significantly higher than that in benign ovarian tumors and healthy normal ovarian tissues and that this was strictly related to the FIGO stage and histological grade. PNMA5 expression in ovarian cancer cell line HO8910 was higher than that in the normal healthy ovarian cell line Moody. PNMA5 knockdown in HO8910 cells not only inhibited the proliferation, migration, invasion, cell cycle, and F-actin polymerization of HO8910 cells but also promoted early apoptosis and led to abnormal distribution and accumulation of mitochondria. PNMA5 phosphorylation was found to be positively regulated by Src activity, and PNMA5 phosphorylation promoted the downstream glycogen synthase kinase-3 β (GSK-3 β) signaling pathway.

Conclusions: PNMA5 plays a pivotal role in the occurrence and development of EOC and is a potential marker of this disease.

Keywords: Epithelial ovarian cancer (EOC); paraneoplastic Ma antigen 5 (PNMA5); HO8910; proliferation; invasion

Submitted Apr 20, 2020. Accepted for publication May 12, 2020.

doi: 10.21037/tcr-20-2013

View this article at: <http://dx.doi.org/10.21037/tcr-20-2013>

Introduction

Ovarian cancer is the most lethal gynecological cancer. Furthermore, 230,000 women will be diagnosed with this condition, and 150,000 will die annually worldwide (1). Advanced epithelial ovarian cancer (EOC) has a 5-year relative survival rate of 29%, in contrast to 92% for early-stage disease (2). The clinical manifestations of EOC are atypical, and effective diagnostic methods at the early stage are lacking. Diagnosis of EOC at an early stage would be extremely beneficial for these patients (3). Therefore, the development of new biochemical markers and therapeutics for EOC is urgently needed (4).

The paraneoplastic Ma antigen (PNMA) family is represented by at least fifteen family members, which are involved in the regulation of growth, apoptosis, or fate determination in different cell types (5). PNMA5 belongs to the PNMA family and has been shown to contain onconeural antigens (6). However, this gene has not been widely studied concerning tumors. Zhou *et al.* concluded that PNMA5 expression is a marker of poor prognosis in patients with metastatic colon cancer (6). Lee *et al.* showed that PNMA5 promotes apoptosis signaling in HeLa and MCF-7 cells and interacts synergistically with MOAP-1 through its N-terminal domain to promote apoptosis and chemosensitivity in human cancer cells (7). Our previous study suggested that PNMA5 is vital for meiosis and is pivotal for the Src→Erk1/2→PNMA5→Akt→glycogen synthase kinase-3β (GSK-3β) signaling pathway (8). These findings indicate that the PNMA5 gene may play an essential role in tumorigenesis and may be a useful therapeutic target. According to our literature review, no study on PNMA5 in ovarian cancer diagnosis and treatment has been conducted to date. Nonetheless, further studies are needed to explore the biological functions and molecular mechanisms of PNMA5 in EOC.

In the present study, we found PNMA5 to be highly expressed in EOC tissues and closely related to the FIGO stage and histological grade. Next confirmed that PNMA5 was highly expressed in the human ovarian cancer cell line HO8910 compared to Moody cells, a normal healthy ovarian cell line. SiRNA technology was then applied to knock down PNMA5 in HO8910 cells, and cell functions were examined. The results suggest that PNMA5 plays a vital role in the occurrence and progression of EOC. Further analyses showed that PNMA5 has a pivotal role in the Src→PNMA5→GSK-3β pathway, though the detailed molecular mechanisms require further study.

Methods

Tissue specimens and cell lines

Fifty ovarian cancer specimens, including 32 serous carcinomas, ten mucinous carcinomas, and eight endometrioid carcinoma samples, were collected from the Second Affiliated Hospital of Nantong University, China from January 2015 to December 2018. Thirty benign ovarian tumor tissue and 20 normal healthy ovarian tissue samples were used as the control group. The age of the patients ranged from 24 to 76 years old. The average ages of the ovarian cancer group, benign ovarian tumor group, and normal healthy ovarian group were 54.98, 48.06, and 50.85 years, respectively. Clinical and pathological data were also collected. The specimens were confirmed by pathological examination. All patients signed an informed consent form, which was approved by the Medical Ethics Committee of the Second Affiliated Hospital of Nantong University (No. KS025). The ovarian cancer cell line HO8910 and the normal healthy ovarian cell line Moody were bought from the Cell Bank of the Chinese Academy of Sciences (Shanghai, China).

Immunohistochemistry

Ovarian cancer, benign ovarian tumor, and normal ovarian tissue specimens were obtained during surgery and fixed in 4% paraformaldehyde, dehydrated with a standard procedure, embedded in paraffin, and sectioned. HE staining was performed, and PNMA5 protein expression was detected by immunohistochemistry using a primary rabbit polyclonal anti-PNMA5 antibody bought from Sigma. The expression levels of PNMA5 were assessed according to both the percentage of positive cells and the staining intensity. The cells were divided into four groups based on the positive cell percentage. Zero points were no positive cells, 1 point was <30% positive cells, 2 points were 30–70% positive cells, and 3 points were >70% positive cells. The cells were subsequently divided into further groups according to the staining intensity. Zero points were no staining, 1 point was positive cells stained pale yellow, 2 points were positive cells stained yellow, and 3 points were positive cells stained brown. The two combined scores were taken as the final result. Zero points (-), 1 to 2 points (+), 3 to 4 points (++), and 5 to 6 points (+++). Furthermore, (-) and (+) were classified as the negative group, and (++) and (+++) were classified as the positive group. These tests were performed in a double-blind manner according

to a standard protocol. Each section was scored by two professional pathologists at the Second Affiliated Hospital of Nantong University, China.

Cell culture

The ovarian cancer cell line HO8910 and the normal ovarian cell line Moody were routinely cultured in DMEM (HyClone) medium containing 10% fetal bovine serum (FBS, HyClone), 100 U/mL penicillin and 100 µg/mL streptomycin (Invitrogen, USA) in a 5% CO₂ incubator at 37 °C.

SiRNA production and transfection

The sequences of all DNA templates for siRNA production are listed (Table S1). One day before transfection, cells (2×10^5) were placed in a six-well plate (Corning, USA) and routinely cultured for 16–20 h to 60–70% confluence. Lipofectamine 3000 reagents (Invitrogen) and DMEM (HyClone) were used for transfection experiments according to the manufacturer's specifications. Next, the transfected cells were collected and analyzed.

Western blot analysis

Cells were lysed, and the collected proteins were separated by sodium dodecyl sulfate polyacrylamide gel electrophoresis (SDS-PAGE) and transferred to polyvinylidene fluoride (PVDF) membranes by a semi-dry transfer method. Primary antibodies were diluted with 5% skim milk powder solution for use and incubated with the membrane at 4 °C overnight. The antibodies included rabbit polyclonal anti-PNMA5 (Sigma), mouse monoclonal anti-GAPDH (Yi Sheng Biotechnology, Ltd, Shanghai, China), rabbit anti-p-PNMA5 (produced by Zhong Ding Biotechnology, Ltd., Nanjing, Jiangsu, China), and rabbit anti-p-GSK-3β (GeneTex, Alton Parkway Irvine, USA). The next day, HRP-labelled anti-rabbit and anti-mouse secondary antibodies (Vazyme, Nanjing, Jiangsu, China) were added and incubated at room temperature for two hours. Signal detection was performed with the enhanced chemiluminescence (ECL) technique using ECL advance reagents (Amersham Biosciences UK, Limited, Little Chalfont Buckinghamshire, England). The results were measured using Image J software.

Cell proliferation assay

The effect of PNMA5 knockdown on cell proliferation was evaluated by the Cell Counting Kit 8 (CCK-8) assay (Nanjing KeyGEN Biotech, Jiangsu, China). Transfected cells at a concentration of 1×10^4 cells/well were seeded into 96-well plates (Corning, USA), after which 10 µL of CCK-8 solution was added to each well, mixed, and incubated for two hours in the dark at 24, 48, 72, 96, and 120 hours. Absorbance, which is positively related to the number of proliferating cells, was measured at 450 nm.

Cell cycle analysis

Twenty-four hours after cell transfection, cells were fixed in precooled absolute ethanol and stored at 4 °C for 24 h, washed twice with PBS and stained with 100 µL of propidium iodide (PI) (concentration 50 µg/mL) (BD) at room temperature for 30 minutes in the dark. The DNA contents of the cells were qualified using a BD FACS Calibur flow cytometer (Becton Dickinson, San Jose, CA, USA). The results were analyzed using FlowJo 2.8 software.

Detection of early apoptosis

Annexin V-FITC/PI double staining (BD) was used. Transfected cells of the knockdown and control groups were collected and stained with 5 µL of Annexin V-FITC solution for 15 minutes and 10 µL of PI solution for 5 minutes at 4 °C in the dark. Images were obtained for early apoptosis analysis.

Cell migration assay

A cell scratch assay was used to evaluate the two-dimensional migration of HO8910 cells. The cells were grown to 80–90% confluence, and a cell-free scratch was generated in each six-well plate with a 10-µL plastic pipette tip. The cell migration of the scratched part was photographed using an inverted microscope (Leica) at 0 h and 48 h, and the healed area in the image was measured using Image J software.

Cell invasion assay

Matrigel invasion chambers (BD) were used for cell invasion

assays. Briefly, 500 μL of DMEM holding 20% FBS was added to the lower chamber, and transfected cells (5×10^4) in serum-free DMEM were seeded in the upper chamber. After incubation for 24 hours at 37 °C, the invasive cells were fixed with neutral formaldehyde and stained with 0.2% crystal violet. Three selected fields were viewed randomly and photographed under a microscope, and absorbance at 570 nm was measured using a microplate reader (Synergy 2, BioTek, USA).

Mitochondrial and F-actin staining

Transfected cells were stained in medium containing 100 nM MitoTracker (Invitrogen TM, USA) for mitochondrial staining and 100 nM rhodamine-phalloidin (Invitrogen TM, USA) for F-actin staining for 20 minutes. 0.3 $\mu\text{g}/\text{mL}$ Hoechst (Bi Yun Tian, Shanghai, China. 1:200 medium dilution) was added for 10 minutes. Photos were obtained using a fluorescence microscope (Eclipse Ti, Nikon, Tokyo, Japan).

Immunofluorescence staining

Cells pretreated with the Src protein inhibitor KX2-391 (20 nM) (Selleck, Houston, Texas, USA) or transfected with PNMA5 siRNA were fixed with paraformaldehyde for 10 minutes at room temperature, and 500 μL of blocking solution [diluted by PBS/PBST, with 10% goat serum (ZSBIO, Beijing, China) and 5% BSA] was added for one hour at 37 °C. Then, 200 μL of primary antibody (1:1,000 dilution ratio of p-PNMA5 or p-GSK-3 β) was added, and the mixture was incubated overnight at 4 °C. Two hundred μL of fluorescent secondary antibody (Cy2-conjugated donkey anti-rabbit IgG, Jackson ImmunoResearch Laboratory, USA) was added for one hour at 37 °C, after which 100 μL of DAPI was added for nuclear staining at room temperature for 10 minutes. Images were acquired using a laser confocal microscope (Eclipse Ti, Nikon, Tokyo, Japan).

Statistical analysis

Statistical analysis was performed using SPSS 17.0 software. Count data are expressed as a percentage (%), and the χ^2 test or Fisher's exact probability method was used. Measurement data are expressed as the mean \pm SD, and *t*-tests were applied. $P < 0.05$ was considered significant.

Results

Expression of PNMA5 is higher in EOC tissues than in benign ovarian tumors and normal ovarian tissues

An earlier study showed that PNMA5 might serve as a marker of poor prognosis in colon cancer and is essential for meiosis. In the present, we aimed to determine whether PNMA5 expression correlates with EOC. Based on immunohistochemistry, PNMA5 expression was observed in the cell cytoplasm and nucleus. The rate of positive PNMA5 expression in EOC tissues was 84.0% (42/50), which was significantly higher than that in benign ovarian tumor tissues (36.7%, 11/30) and normal ovarian tissues (35%, 7/20), the difference was statistically significant ($\chi^2 = 18.788$, $P < 0.001$ and $\chi^2 = 16.333$, $P < 0.001$) (Table 1, Figure 1).

The relationship between PNMA5 expression in EOC and clinicopathological features

To investigate the relationship between PNMA5 expression in EOC and clinicopathological features, we grouped the clinical and pathological data for 50 EOC cases according to age, International Federation of Gynecology and Obstetrics (FIGO) 2014 stage, histological grade, and the pathological type and analyzed PNMA5 expression in these groups. The results showed a rate of positive PNMA5 expression in stage I–II EOC tissues of 70.83% (17/24), which was lower than that of stage III–IV tissues (96.15%, 25/26), the difference was statistically significant ($\chi^2 = 5.953$, $P < 0.05$). The positive expression rate of PNMA5 in EOC patients with high-medium differentiation (G1–G2) was 71.43% (15/21), lower than that of patients with poor differentiation (G3) (93.10%, 27/29), the difference was statistically significant ($\chi^2 = 4.258$, $P < 0.05$) (Table 2).

PNMA5 knockdown inhibits proliferation, blocks the cell cycle and promotes early apoptosis in HO8910 cells

Western blot results showed that PNMA5 expression in HO8910 cells was significantly higher than that in Moody cells (Figure 2A,B). We knocked down PNMA5 expression in HO8910 cells by siRNA to further explore the biological functions of PNMA5 in ovarian cancer. The knockdown efficiency was confirmed by western blot (Figure 2C,D). CCK-8 assay revealed that the proliferation of HO8910 in the knockdown group was lower than that in the

Table 1 PNMA5 expression in ovarian cancer, benign ovarian tumor, and normal healthy ovarian tissues

Groups	n	Positive expression	Positive expression rate (%)	χ^2	P
Ovarian cancer	50	42	84.0	18.788	<0.001 ^a
Benign ovarian tumors	30	11	36.7	0.015	0.904 ^b
Normal ovary	20	7	35.0	16.333	<0.001 ^c

There was a statistically significant difference among the three groups ($\chi^2=24.0139$, $P<0.001$). ^a, compared with the benign ovarian tumor tissue; ^b, compared with normal healthy ovarian tissue; ^c, compared with ovarian cancer tissue. PNMA5, paraneoplastic Ma antigen 5.

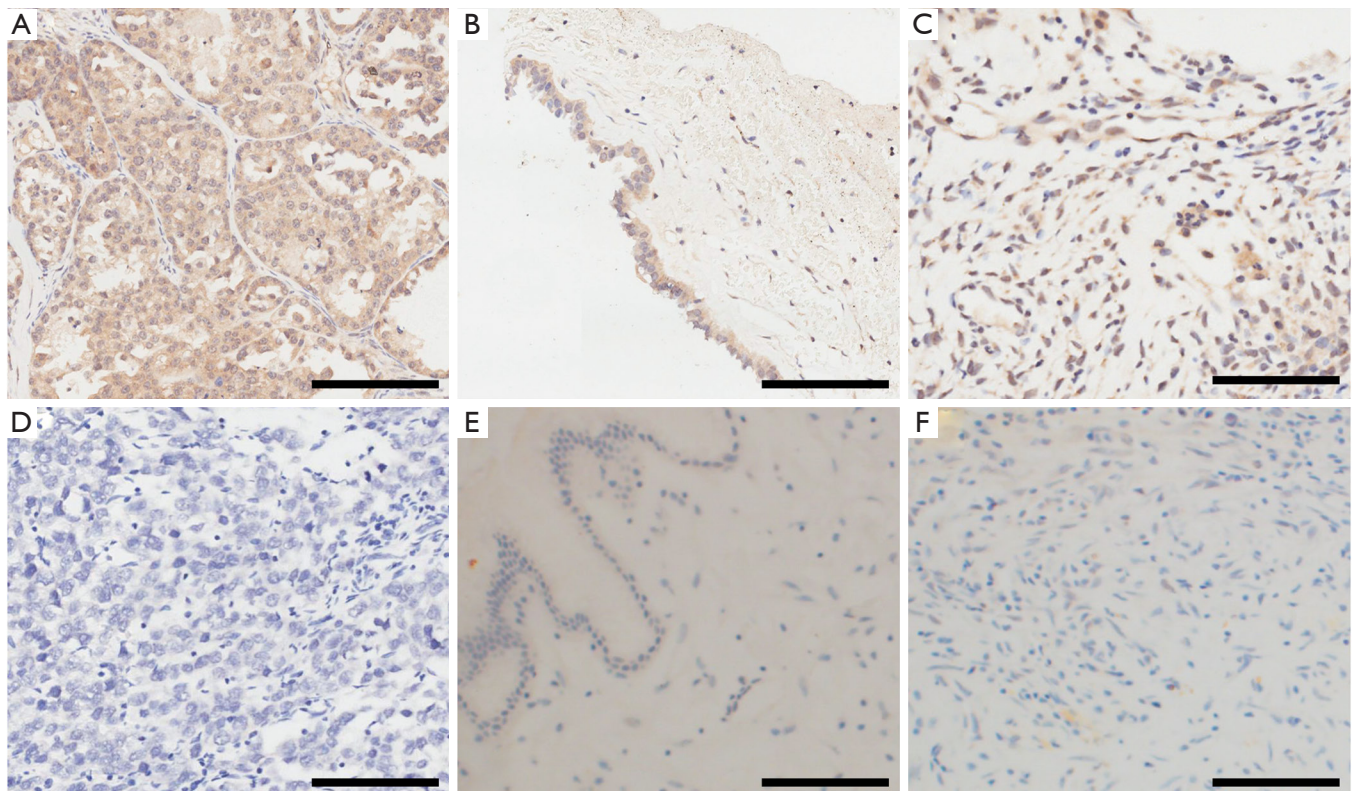


Figure 1 The representative images of the PNMA5 expression done by IHC. The expression levels of PNMA5 were judged according to a protocol that showed in the “Methods” section. (A) High expression in ovarian cancer tissue. (B) Positive expression in benign ovarian tumor tissue. (C) Positive expression in normal ovarian tissue. (D) Negative expression in ovarian cancer tissue. (E) Negative expression in ovarian benign tumor tissue. (F) Negative expression in normal ovarian tissue. Bar =100 μ m). PNMA5, paraneoplastic Ma antigen 5.

control group on day two and day three. Furthermore, similar results were observed on the fourth and fifth days, indicating a stable plateau (Figure 2E). PI staining followed by flow cytometry showed that the G1 phase percentage of HO8910 cells in the knockdown group was higher than that in the control group, and the percentage of cells in S phase decreased significantly (Figure 2F,G). Annexin V-FITC/PI double staining revealed that the early apoptotic rate of HO8910 in the knockdown group was significantly higher

than that in the control group (Figure 2H,I).

PNMA5 knockdown leads to abnormal distribution of the mitochondria, inhibits the migration, invasion and F-actin polymerization in HO8910 cells

Mitochondrial function is an essential indicator of cell quality. Immunofluorescence labeling via MitoTracker staining showed that mitochondria were evenly distributed

Table 2 Relationship between the expression of PNMA5 in epithelial ovarian cancer tissues and the clinicopathological characteristics

Clinicopathological characteristics	n	PNMA5 (+)	PNMA5 (-)	χ^2	P
Age				2.009	0.156
>50	30	27	3		
≤50	20	15	5		
FIGO stage [2014]				5.953	0.015
I-II	24	17	7		
III-IV	26	25	1		
Histological grade				4.258	0.039
G1-G2	21	15	6		
G3	29	27	2		
Tumor type				0.893	0.640
Serous	32	28	4		
Mucinous	10	8	2		
Endometrioid	8	6	2		

PNMA5, paraneoplastic Ma antigen 5.

in the cytoplasm of the control group but were sporadically and unevenly distributed in the knockdown group. There was no significant difference in nuclear morphology between the two groups (*Figure 3A*). Quantification of fluorescence intensity revealed significantly higher levels in the knockdown group than in the control group (*Figure 3B*). Cell scratch assays and Transwell assays were used to detect the two-dimensional migration (*Figure 3C,D*) and invasion (*Figure 3E,F*), respectively, of HO8910 cells, with the results showing that both were significantly lower in the knockdown group than in the control group. F-actin is a vital part of the cytoskeleton and plays a crucial role in the cellular movement. Immunofluorescence labeling with rhodamine-phalloidin revealed abundant microfilaments with a regular arrangement. Additionally, the fluorescence intensity was significantly enhanced in the control group but lower in the knockdown group. As with MitoTracker staining, there was no significant difference in nuclear morphology between the two groups based on rhodamine-phalloidin (*Figure 3G*). Immunofluorescence quantification showed that the fluorescence signal in the knockdown group was significantly weaker than that in the control group (*Figure 3H*).

Phosphorylation of PNMA5 is positively regulated by Src activity, and PNMA5 positively regulates downstream phosphorylated GSK-3 β

Our previous study confirmed the activity of the PNMA5 signaling pathway (Src→Erk1/2→PNMA5→Akt→GSK-3 β), and the phosphorylation level of PNMA5 was related to upstream Src and Erk1/2 (8). In this study, HO8910 cells were treated with a Src protein inhibitor, and expression of PNMA5 and p-PNMA5 was detected by western blot analyses. There was no difference in total PNMA5 expression, though the level of p-PNMA5 in the Src inhibition group was significantly lower than that in the control group (*Figure 4A,B*). According to immunofluorescence analysis, the fluorescence signal of p-PNMA5 in HO8910 cells in the Src inhibition group was significantly weaker than that in the control group (*Figure 4C,D*). We also used western blot and immunofluorescence analyses to detect p-GSK-3 β levels downstream of PNMA5 in HO8910 cells. Western blotting showed significantly decreased levels of p-GSK-3 β in the knockdown group compared with the control group, though GSK-3 β expression was unchanged (*Figure 4E,F*).

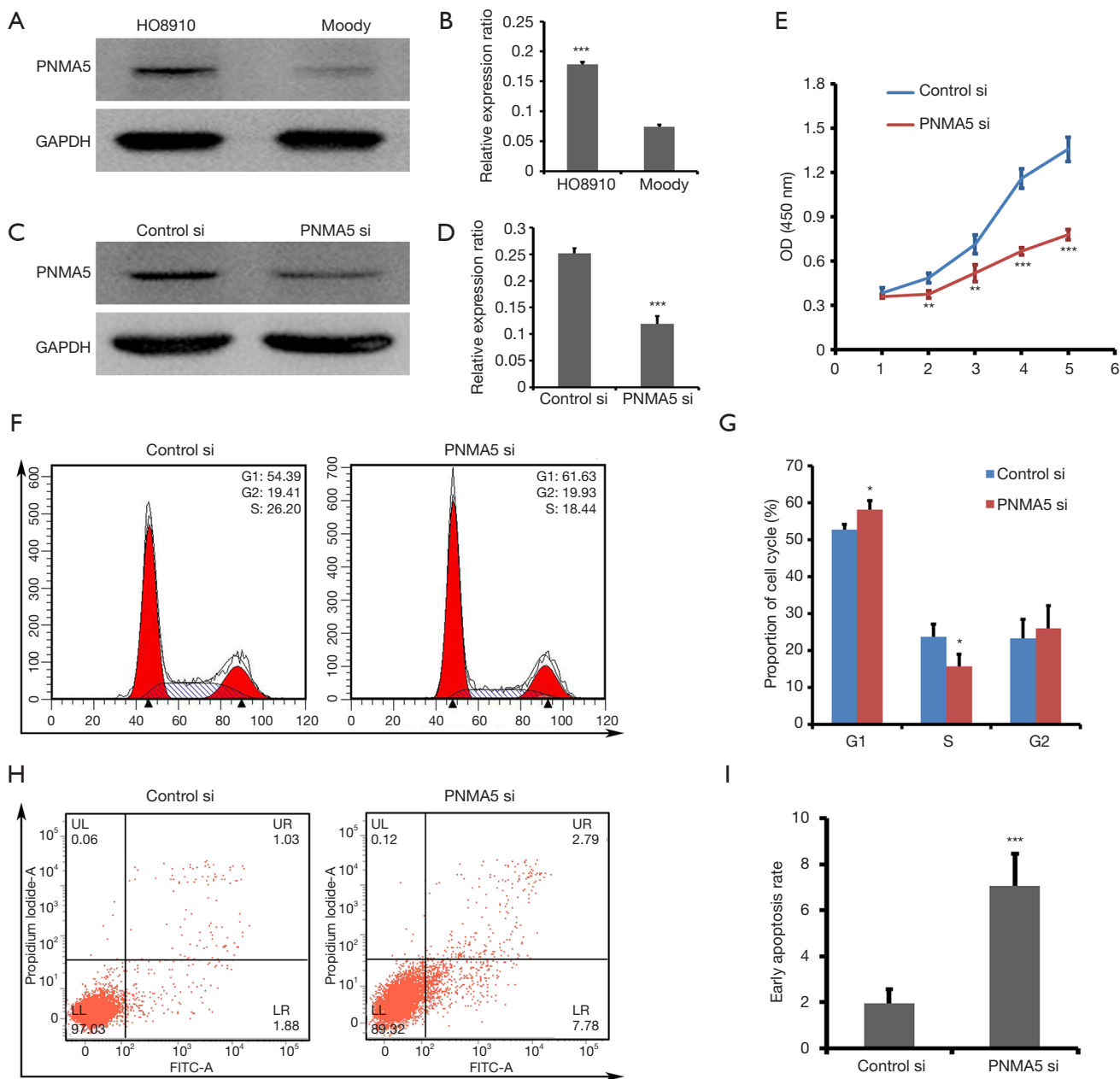
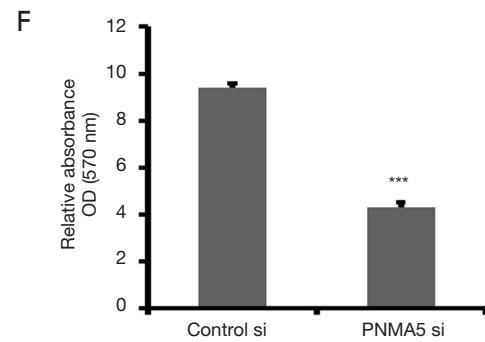
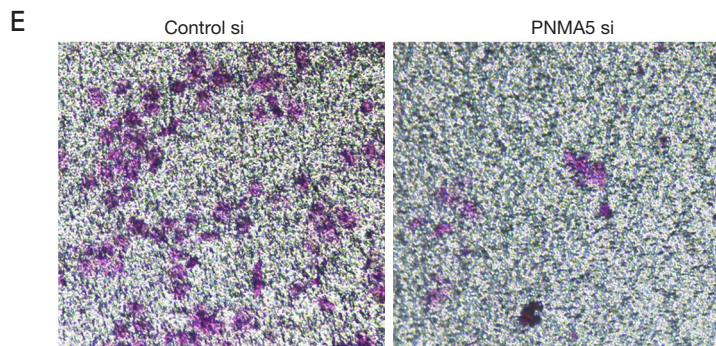
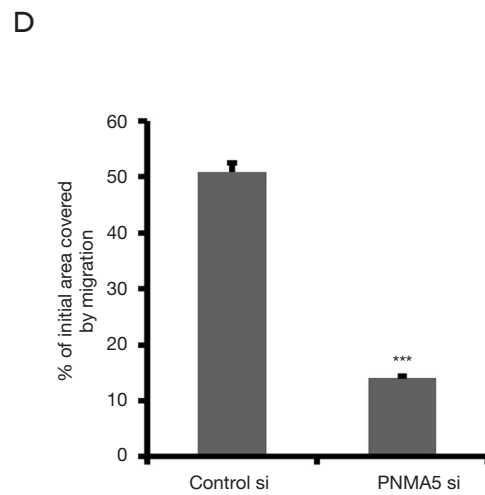
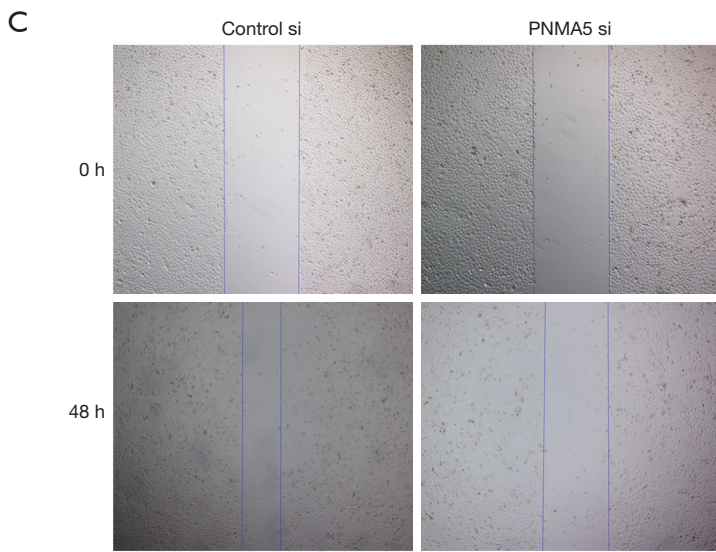
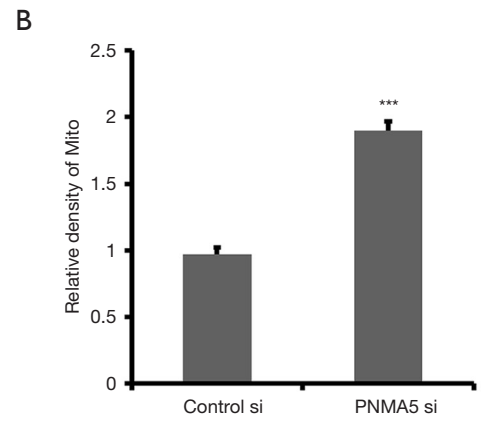
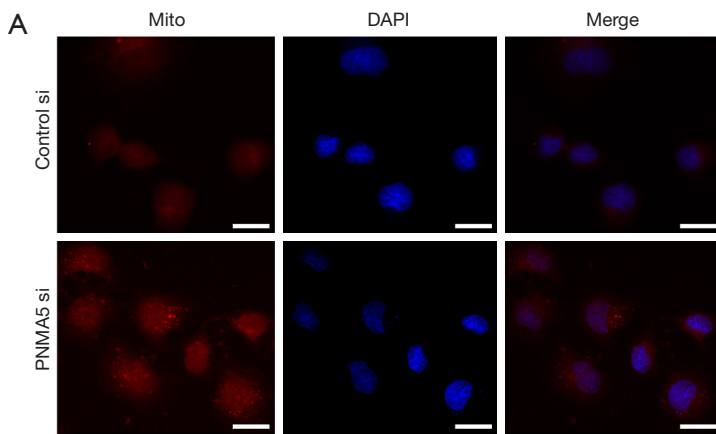


Figure 2 PNMA5 knockdown inhibited the proliferation, blocked the cell cycle, and promoted early apoptosis of HO8910 cells. (A,B) Western blot showed that PNMA5 was higher expressed in HO8910 than in Moody. (C,D) The expression of PNMA5 in the PNMA5 siRNA group was significantly lower than that in the control siRNA group. (E) CCK-8 showed that PNMA5 knockdown inhibited the proliferation of HO8910 cells. (F,G) PI staining showed that the PNMA5 knockdown blocked the cell cycle. (H,I) Annexin V-FITC/PI double staining revealed that the PNMA5 knockdown promoted early apoptosis of HO8910. n=3, *P<0.05, **P<0.01, ***P<0.001. PNMA5, paraneoplastic Ma antigen 5; CCK-8, Cell Counting Kit 8.



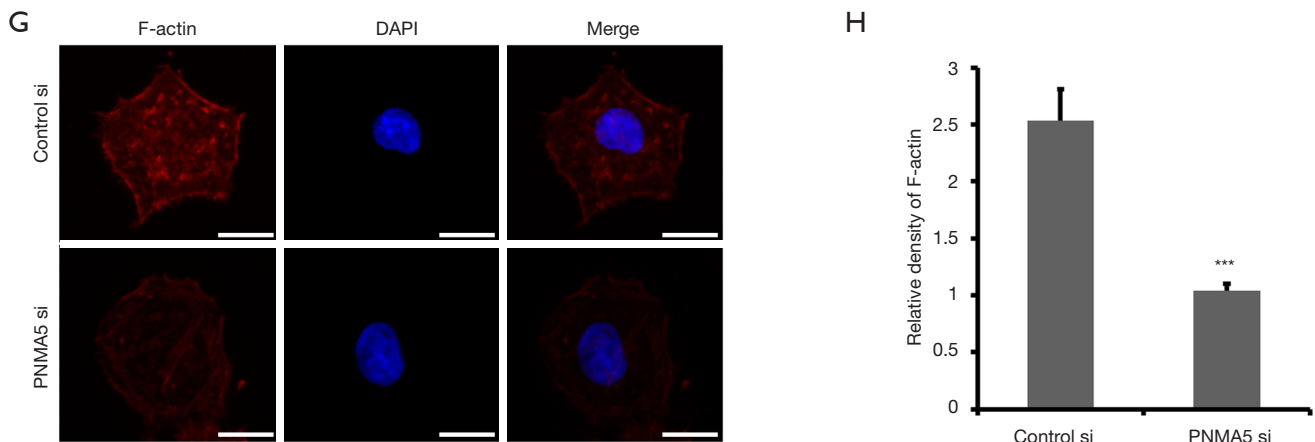


Figure 3 PNMA5 knockdown led to abnormal distribution of the mitochondria, inhibited the migration, invasion, and F-actin Polymerization in HO8910 Cells. (A) The mitochondria were evenly distributed in the cytoplasm in the control group but spotted and unevenly distributed in the knockdown group. Scale bar, 50 μm . (B) Quantification analysis of the fluorescence intensity of the mitochondria. (C,D) PNMA5 knockdown inhibited the migration and (E,F) invasion of HO8910 cells. (G) The F-actin was highly expressed with a regular organization, and the fluorescence intensity was significantly enhanced in the control group but attenuated in the knockdown group. Scale bar, 50 μm . (H) Quantification analysis of the fluorescence intensity of the microfilaments. $n=3$, *** $P<0.001$. PNMA5, paraneoplastic Ma antigen 5.

Immunofluorescence analysis also showed significantly lower levels of p-GSK-3 β in the knockdown group than in the control group (Figure 4G,H). The above results suggest that PNMA5 phosphorylation is positively regulated by Src activity and that PNMA5 exerts its biological effects by positively regulating downstream phosphorylated GSK-3 β .

Discussion

Extensive efforts have been made to implement screening of the general population for early diagnosis of EOC, but there is currently no approved strategy (9). Based on a genome-wide study, PNMA5 is thought to be a female fertility factor (10). To date, there have been no studies on PNMA5 in EOC. In the present study, we observed that PNMA5 was highly expressed in EOC and HO8910 cells and that positive expression of PNMA5 in EOC was closely related to the FIGO stage and histological grade. These results show that PNMA5 may play a vital role in the development and progression of EOC.

The study has shown that the most fundamental trait of cancer cells involves the ability to sustain chronic proliferation (11), and thus attenuating the proliferative signaling can inhibit cancer cell proliferation. Our experiments showed that knockdown of PNMA5 could inhibit cell proliferation of the HO8910 cell line

significantly, showing a crucial role of PNMA5 in HO8910 cell proliferation. The previous study showed that cell proliferation was regulated by the cell cycle progression (12). Our flow cytometric analyses showed that knockdown of PNMA5 blocked the G1/S-phase transition of HO8910 cells, similar to the findings of Yan (13). Furthermore, our apoptosis analysis indicated that PNMA5 knockdown significantly promoted apoptosis in HO8910 cells, which is different from what Lee *et al.* have reported (7), and may be a result of different kind of cell lines to be used. These results reveal that PNMA5 may play a key role in increasing HO8910 cell proliferation and suppressing apoptosis, which may further promote the development and progression of EOC.

Molecular evidence also suggests that the deregulation of mitochondrial biogenesis, morphology, dynamics, and apoptosis is involved in carcinogenesis (14). Recent data show that mitochondria are functional in many cancer cells, and they contribute, together with glycolysis, to sustain cell proliferation. According to our results, knockdown of PNMA5 leads to abnormal distribution and aggregation of mitochondria, and the change in morphology may affect the function of mitochondria in HO8910 cells, resulting in an increased apoptosis rate and decreased proliferation.

High invasiveness is one characteristic of EOC, and advanced EOC more inclined to invasion and metastasis

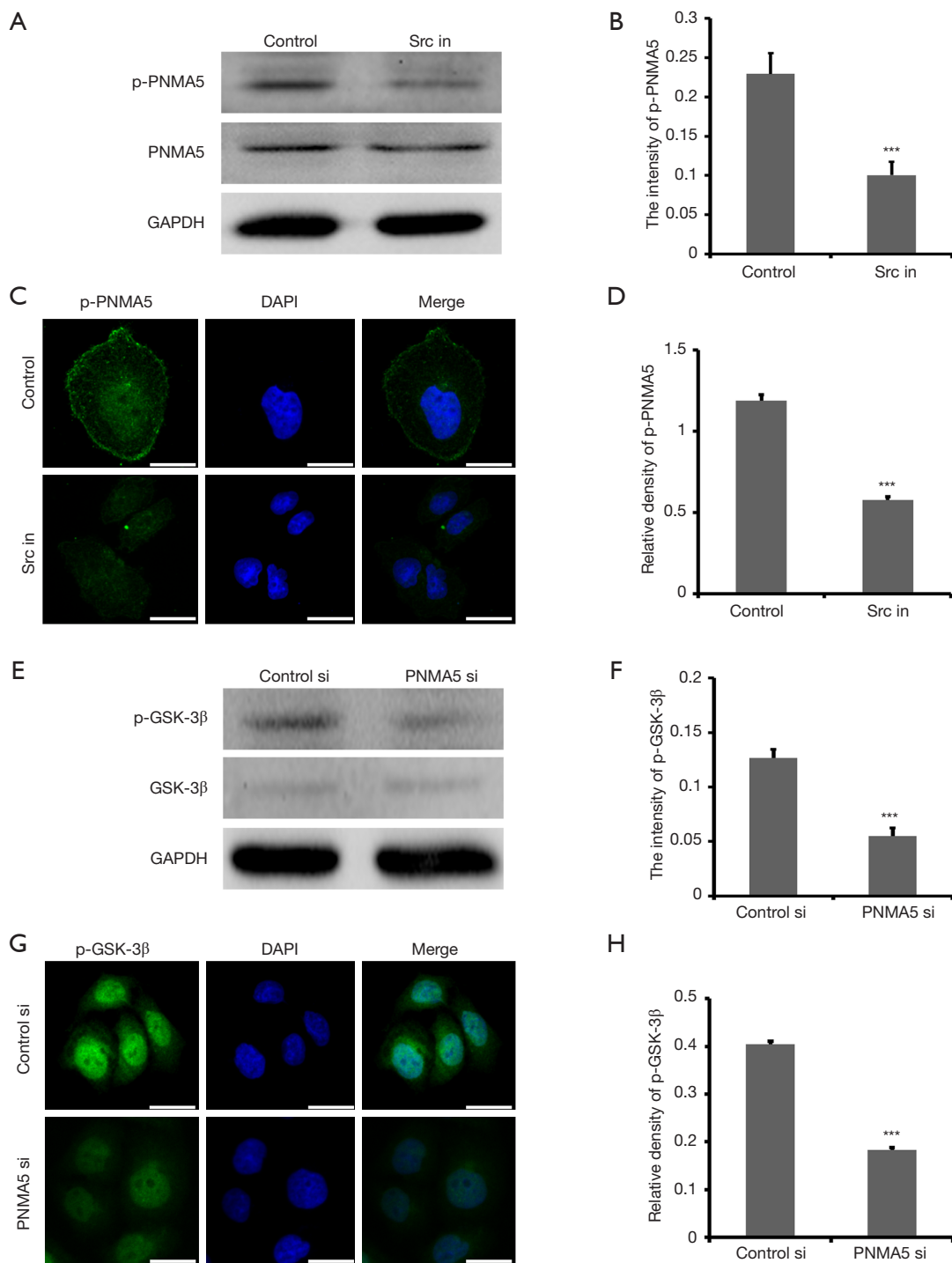


Figure 4 Phosphorylation of PNMA5 was positively regulated by Src activity, and PNMA5 positively regulated downstream phosphorylated GSK-3 β . (A,B) Western blot analysis showed the expression of PNMA5 and p-PNMA5 in HO8910 cells pretreated with a Src inhibitor. (C,D) Immunofluorescence analysis showed that the fluorescence signal of p-PNMA5 in HO8910 cells pretreated with Src inhibitor. Scale bar, 50 μ m. (E,F) Western blot analysis showed the expression of p-GSK-3 β and GSK-3 β in HO8910 cells after PNMA5 knockdown. (G,H) Immunofluorescence analysis showed the p-GSK-3 β expression in HO8910 cells after the PNMA5 knockdown. Scale bar, 50 μ m. n=3, ***P<0.001. PNMA5, paraneoplastic Ma antigen 5; GSK-3 β , glycogen synthase kinase-3 β .

early. Migration is an essential step during this process (15). The stronger the migration ability, the more extensive the invasion, and metastasis ability EOC shows (16,17). Our results showed that knockdown of PNMA5 significantly suppressed the migration and invasion of HO8910 cells, which reveal that PNMA5 is involved in the migration and invasion, and plays a vital role in the process of metastasis in EOC. Cell migration and invasion rely on polymerization and stretching of the actin filament (18,19), and driven by specific protrusive and contractile actin filament structures (20). The cytoskeleton is regulated by corresponding cell signals (21). Ohishi *et al.* reported tankyrase-binding protein (TNKS1BP1) regulated actin cytoskeleton rearrangement and cancer cell invasion (22). Our results showed that microfilaments decreased in abundance after knocking down PNMA5 in HO8910. The results show that PNMA5 knockdown inhibits actin in HO8910, and then results in the delay of cell migration and invasion. In other words, PNMA5 may promote microfilament synthesis to accelerate migration and invasion of ovarian cancer cells and cause tumor metastasis.

Src-family kinases (SFKs), which are involved in oncogenesis, are implicated in the promotion of tumor cell motility, proliferation, inhibition of apoptosis, invasion, and metastasis (23). Our previous study confirmed the phosphorylation level of PNMA5 was related to upstream Src and Erk1/2 (8). In this study, we used Src inhibitors to clarify the relationship between Src and PNMA5 in HO8910 cells and found that levels of phosphorylated PNMA5 decreased dramatically, with no change in PNMA5. Our results are consistent with our earlier study, further confirms that the Src gene is upstream of PNMA5 and that phosphorylated PNMA5 is positively regulated by Src activity.

The “hyperactivation” of GSK-3 β may have oncogenic effects in several types of human cancers, including colon cancer (24), hepatocellular carcinomas (25), and gastric cancer (26). In this study, we found that phosphorylated GSK-3 β was significantly downregulated but that GSK-3 β was unchanged in HO8910 cells after PNMA5 knockdown. These results show that the *PNMA5* gene is upstream of GSK-3 β and that phosphorylated PNMA5 can positively regulate the GSK-3 β pathway.

In conclusion, to the best of our knowledge, the present study is the first to investigate PNMA5 function in EOC tissues and cell lines, and our results suggest that PNMA5 plays a vital role in the occurrence and development of EOC and is a potential biomarker for this disease. Further

studies are still needed to explore the biological functions of PNMA5 and the precise underlying mechanisms, and our study should be confirmed *in vitro* and *in vivo* in future investigations.

Acknowledgments

The language of the manuscript was edited by American Journal of Experts (AJE).

Funding: The current study was supported by grants from the Science and Technology Bureau of Nantong, Jiangsu, China (Grant No. MS12018009).

Footnote

Data Sharing Statement: Available at <http://dx.doi.org/10.21037/tcr-20-2013>

Conflicts of Interest: All authors have completed the ICMJE uniform disclosure form (available at <http://dx.doi.org/10.21037/tcr-20-2013>). The authors have no conflicts of interest to declare.

Ethical Statement: The authors are accountable for all aspects of the work in ensuring that questions related to the accuracy or integrity of any part of the work are appropriately investigated and resolved. The study was approved by the Medical Ethics Committee of the Second Affiliated Hospital of Nantong University (No. KS025). All patients signed an informed consent form for the study.

Open Access Statement: This is an Open Access article distributed in accordance with the Creative Commons Attribution-NonCommercial-NoDerivs 4.0 International License (CC BY-NC-ND 4.0), which permits the non-commercial replication and distribution of the article with the strict proviso that no changes or edits are made and the original work is properly cited (including links to both the formal publication through the relevant DOI and the license). See: <https://creativecommons.org/licenses/by-nc-nd/4.0/>.

References

1. Ferlay J, Soerjomataram I, Dikshit R, et al. Cancer incidence and mortality worldwide: sources, methods and major patterns in GLOBOCAN 2012. *Int J Cancer* 2015;136:E359-86.
2. Reid BM, Permuth JB, Sellers TA. Epidemiology of

- ovarian cancer: a review. *Cancer Biol Med* 2017;14:9-32.
3. Jelovac D, Armstrong DK. Recent progress in the diagnosis and treatment of ovarian cancer. *CA Cancer J Clin* 2011;61:183-203.
 4. Jaragh-Alhadad L. In-vitro evaluation of HSP27 inhibitors function through HER2 pathway for ovarian cancer therapy. *Transl Cancer Res* 2018;7:1510-7.
 5. Pang SW, Lahiri C, Poh CL, et al. PNMA family: Protein interaction network and cell signalling pathways implicated in cancer and apoptosis. *Cell Signal* 2018;45:54-62.
 6. Zhou Y, Zang Y, Yang Y, et al. Candidate genes involved in metastasis of colon cancer identified by integrated analysis. *Cancer Med* 2019;8:2338-2347.
 7. Lee YH, Pang SW, Poh CL, et al. Distinct functional domains of PNMA5 mediate protein-protein interaction, nuclear localization, and apoptosis signaling in human cancer cells. *J Cancer Res Clin Oncol* 2016;142:1967-77.
 8. Zhang XL, Liu P, Yang ZX, et al. PNMA5 is essential to the progression of meiosis in mouse oocytes through a chain of phosphorylation. *Oncotarget* 2017;8:96809-25.
 9. Menon U, Karpinskyj C, Gentry-Maharaj A. Ovarian cancer prevention and screening. *Obstet Gynecol* 2018;131:909-27.
 10. Gallardo TD, John GB, Shirley L, et al. Genomewide discovery and classification of candidate ovarian fertility genes in the mouse. *Genetics* 2007;177:179-94.
 11. Hanahan D, Weinberg RA. Hallmarks of cancer: the next generation. *Cell* 2011;144:646-74.
 12. Wang D, Sun SQ, Yu YH, et al. Suppression of SCIN inhibits human prostate cancer cell proliferation and induces G0/G1 phase arrest. *Int J Oncol* 2014;44:161-6.
 13. Yan T, Liang W, Jiang E, et al. GINS2 regulates cell proliferation and apoptosis in human epithelial ovarian cancer. *Oncol Lett* 2018;16:2591-8.
 14. Signorile A, De Rasio D, Cormio A, et al. Human Ovarian Cancer Tissue Exhibits Increase of Mitochondrial Biogenesis and Cristae Remodeling. *Cancers (Basel)* 2019;11:1350.
 15. Takai M, Terai Y, Kawaguchi H, et al. The EMT (epithelial-mesenchymal-transition)-related protein expression indicates the metastatic status and prognosis in patients with ovarian cancer. *J Ovarian Res* 2014;7:76-83.
 16. Chen Q, Liu X, Xu L, et al. Long non-coding RNA BACE1-AS is a novel target for anisomycin-mediated suppression of ovarian cancer stem cell proliferation and invasion. *Oncol Rep* 2016;35:1916-24.
 17. Zhang W, Liu R, Tang C, et al. PFTK1 regulates cell proliferation, migration and invasion in epithelial ovarian cancer. *Int J Biol Macromol* 2016;85:405-16.
 18. Zhao X, Jiang M, Wang Z. TPM4 promotes cell migration by modulating F-actin formation in lung cancer. *Oncotargets Ther* 2019;12:4055-63.
 19. Li Y, Li X, Liu KR, et al. Visfatin derived from ascites promotes ovarian cancer cell migration through Rho/ROCK signaling-mediated actin polymerization. *Eur J Cancer Prev* 2015;24:231-9.
 20. Lehtimäki J, Hakala M, Lappalainen P. Actin Filament Structures in Migrating Cells. *Handb Exp Pharmacol* 2017;235:123-52.
 21. Peng JM, Bera R, Chiou CY, et al. Actin cytoskeleton remodeling drives epithelial-mesenchymal transition for hepatoma invasion and metastasis in mice. *Hepatology* 2018;67:2226-43.
 22. Ohishi T, Yoshida H, Katori M, et al. Tankyrase-Binding Protein TNKS1BP1 Regulates Actin Cytoskeleton Rearrangement and Cancer Cell Invasion. *Cancer Res* 2017;77:2328-38.
 23. Zhang S, Yu D. Targeting Src family kinases in anti-cancer therapies: turning promise into triumph. *Trends Pharmacol Sci* 2012;33:122-8.
 24. Salim T, Sjölander A, Sand-Dejmek J. Nuclear expression of glycogen synthase-3 β and lack of membranous β -catenin is correlated with poor survival in colon cancer. *Int J Cancer* 2013;133:807-15.
 25. Cervello M, Augello G, Cusimano A, et al. Pivotal roles of glycogen synthase-3 in hepatocellular carcinoma. *Adv Biol Regul* 2017;65:59-76.
 26. Hua K, Li Y, Zhao Q, et al. Downregulation of Annexin A11 (ANXA11) Inhibits Cell Proliferation, Invasion, and Migration via the AKT/GSK-3 β Pathway in Gastric Cancer. *Med Sci Monit* 2018;24:149-60.

Cite this article as: Qiao H, Liu J, Yang Z, Gao L, Zhang X, Lu G, Liu Y, Liu M, Ying X, Zhang D. PNMA5 knockdown suppresses the proliferation, invasion, and metastasis of epithelial ovarian cancer cells. *Transl Cancer Res* 2020;9(5):3691-3702. doi: 10.21037/tcr-20-2013

Supplementary

Table S1 DNA templates for siRNA production

Target site	DNA templates
159-179 ¹	Oligo1: GGATCCTAATACGACTCACTATAGAGAATGTTTCAGGAGGGAAGA ² Oligo2: AATCTTCCCTCCTGAACATTCTCTATAGTGAGTCGTATTAGGATCC ² Oligo3: GATCCTAATACGACTCACTATATCTTCCCTCCTGAACATTCTC ² Oligo4: AAGAGAATGTTTCAGGAGGGAAGATATAGTGAGTCGTATTAGGATCC ²
295-315 ¹	Oligo1: GGATCCTAATACGACTCACTATAGATGATGAGTTTCTCAGTAGA ² Oligo2: AATCTACTGAGAACTCATCATCTATAGTGAGTCGTATTAGGATCC ² Oligo3: GATCCTAATACGACTCACTATATCTACTGAGAACTCATCATC ² Oligo4: AAGATGATGAGTTTCTCAGTAGATATAGTGAGTCGTATTAGGATCC ²
442-462 ¹	Oligo1: GGATCCTAATACGACTCACTATAGAGCCTCCGAAAGAAAGTATG ² Oligo2: AACATACTTTCTTTTCGGAGGCTCTATAGTGAGTCGTATTAGGATCC ² Oligo3: GATCCTAATACGACTCACTATACATACTTTCTTTTCGGAGGCTC ² Oligo4: AAGAGCCTCCGAAAGAAAGTATGTATAGTGAGTCGTATTAGGATCC ²
718-738 ¹	Oligo1: GGATCCTAATACGACTCACTATAGACTTTAGAGCCTCTCAGTTT ² Oligo2: AAAAAGTAAAGTCTATAGTGAGTCGTATTAGGATCC ² Oligo3: GGATCCTAATACGACTCACTATAAAAAGTAAAGTCTAAAGTC ² Oligo4: AAGACTTTAGAGCCTCTCAGTTTATAGTGAGTCGTATTAGGATCC ²
Control ³	Oligo1: GGATCCTAATACGACTCACTATAGACCTACGCCACCAATTCGT ² Oligo2: AAACGAAATTGGTGGCGTAGGTCTATAGTGAGTCGTATTAGGATCC ² Oligo3: GGATCCTAATACGACTCACTATAACGAAATTGGTGGCGTAGGTC ² Oligo4: AAGACCTACGCCACCAATTCGTTATAGTGAGTCGTATTAGGATCC ²

¹, the numbers are the starting and ending positions of the target sites in PNMA5 CDS. ², two pairs of DNA oligos are needed for each double-strand siRNA. Oligo 2 is complementary with oligo one except for an "AA" overhang at 5'. Oligo 4 is complementary with oligo three except an "AA" overhang at 5'. In each oligo, gene-specific sequences are underlined. The other sequences are for recognition and binding by T7 RNA polymerase. ³, control siRNA does not target any mRNA sequence in humans. PNMA5, paraneoplastic Ma antigen 5.